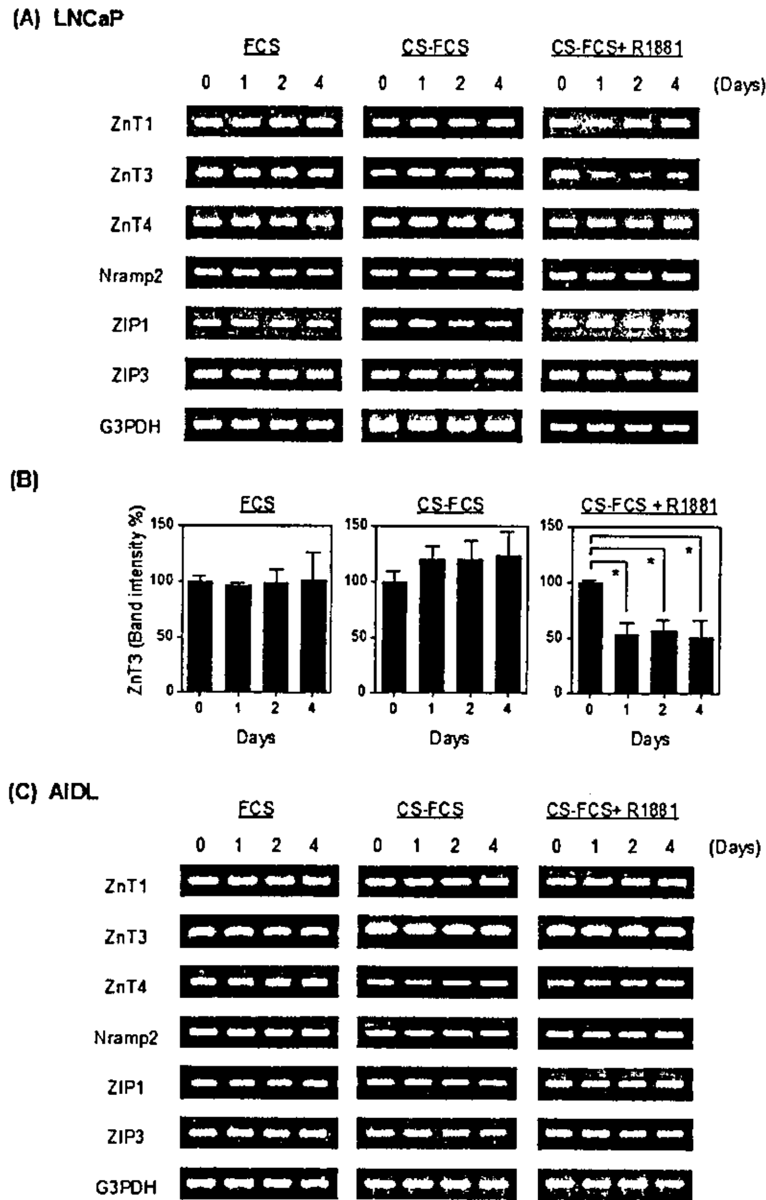

Figure 5. Effect of androgen on mRNA expression of zinc transporters in LNCaP and AIDL cells. (A) LNCaP cells were cultured in phenol red-free RPMI-1640 supplemented with 2% fetal calf serum (FCS) for 3 d, and then the culture medium was replaced with the medium containing FCS or charcoal-stripped (CS)-FCS with or without 100 nM R1881. After incubation, total RNA was isolated and subjected to reverse transcriptase polymerase chain reaction (RT-PCR)analysis. The products were resolved on 1.75% agarose gels and visualized with ethidium bromide. (B) Band intensity was quantified using the National Institutes of Health Image program. The intensities of ZnT3 were normalized with glyceraldehyde-3-phosphate dehydrogenase and expressed as a percentage of the value of day 0. Values represent the means ± SD from 3 different experiments. * indicates $P < .05$ vs day 0 (Scheffe's test). (C) AIDL cells were treated with the same conditions as described in (A). After incubation, total RNA was isolated and subjected to RT-PCR analysis. The products were resolved on 1.75% agarose gels and visualized with ethidium bromide.

which is generated to be cultured in the medium containing 2% hormone-stripped FCS, may partially result from its culture condition.

The high-level expression of ZnT3 was observed in LNCaP cells cultured in hormone-reduced medium. It is not clear from our experiments whether the increased expression of ZnT3 is mediated directly by hormone ablation or indirectly through alterations of environmental androgen. Although an androgen response element was not found in the 5′ promoter region of ZnT3 gene [data not shown; the sequence was described in the GenBank database (accession number NT_022184)], since cis-element

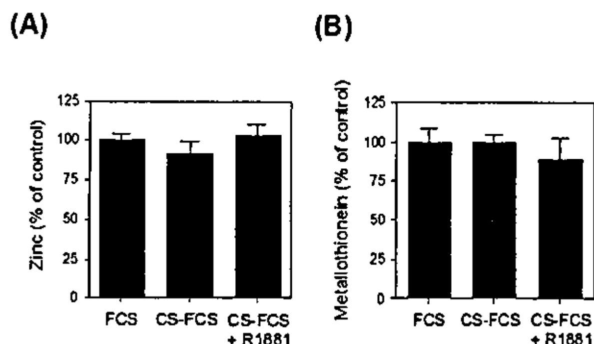

Figure 6. Effects of androgen on zinc and metallothionein levels in LNCaP cells. LNCaP cells were treated under the same conditions as described in Figure 5 (A). After 4 d of incubation, intracellular zinc (A) and metallothionein (B) levels were determined. Values represent the means ± SD from 3 incubations.

sequence that is required to mediate a negative regulation by androgen is almost unknown, the unidentified androgen response element may exist in the upstream region of the ZnT3 gene. We are going to further investigate the transcriptional regulation of the ZnT3 gene.

Expression of metallothionein in rat prostate is known to be regulated by androgen, but the degree of the androgenic effect is different among lobes of prostate (Ghatak et al, 1996; Tohyama et al, 1996; Yamashita et al, 1996). The rat prostate consists of at least 3 anatomically independent lobes, designated as the ventral, lateral, and dorsal prostate. In ventral prostate, metallothionein expression was not detectable and castration appeared to induce metallothionein gene expression, but testosterone administration after castration had no effect on the expression (Tohyama et al, 1996). In dorsolateral prostate, metallothionein was present and testosterone caused a reversal of the effect of castration on metallothionein induction (Ghatak et al, 1996; Tohyama et al, 1996). In lateral prostate, metallothionein expression was not regulated by androgen (Yamashita et al, 1996). These findings suggest that metallothionein gene expression is regulated by androgen in the dorsal prostate, but not lateral and ventral prostate. LNCaP cells have been reported to exhibit the characteristics of lateral prostate cells (Costello et al, 1999); therefore, our observation of no effect on metallothionein expression in LNCaP cells by androgen supports the previous studies.

In conclusion, we first showed that the expression of ZnT3 mRNA underwent an androgenic regulation in LNCaP cells and the high-level expression of ZnT3 mRNA was detected in the androgen-independent subline derived from LNCaP cells. In addition, high levels of ZnT1 and low levels of metallothionein were detected in AIDL cells. The elucidation of the relation between the expressions of ZnT1, ZnT3, and metallothionein and the progression of prostate cancer to the hormone-refractory state might help in understanding the physiology of prostate cancer.

References

Andrews GK. Cellular zinc sensors: MTF-1 regulation of gene expression. *Biometals.* 2001;14:223–237.

Beyersmann D, Haase H. Functions of zinc in signaling, proliferation and differentiation of mammalian cells. *Biometals.* 2001;14:331–341.

Cole TB, Wenzel HJ, Kafer KE, Schwartzkroin PA, Palmiter RD. Elimination of zinc from synaptic vesicles in the intact mouse brain by disruption of the ZnT3 gene. *Proc Natl Acad Sci U S A.* 1999;96:1716–1721.

Costello LC, Franklin RB. Aconitase activity, citrate oxidation, and zinc inhibition in rat ventral prostate. *Enzyme.* 1981;26:281–287.

Costello LC, Liu Y, Franklin RB, Kennedy MC. Zinc inhibition of mitochondrial aconitase and its importance in citrate metabolism of prostate epithelial cells. *J Biol Chem.* 1997;272:28875–28881.

Costello LC, Liu Y, Zou J, Franklin RB. Evidence for a zinc uptake transporter in human prostate cancer cells which is regulated by prolactin and testosterone. *J Biol Chem.* 1999;274:17499–17504.

Cousins RJ. Absorption, transport, and hepatic metabolism of copper and zinc: special reference to metallothionein and ceruloplasmin. *Physiol Rev.* 1985;65:238-309.

Emmett JL, Green LF, Papantonious A. Endocrine therapy in carcinoma of the prostate gland: 10-year survival studies. *J Urol.* 1960;83:471–484.

Fair WR, Couch J, Wehner N. Prostatic antibacterial factor. *Urology.* 1976;7:169–177.

Fair WR, Parrish RF. Antibacterial substances in prostatic fluid. *Prog Clin Biol Res.* 1981;75:247–264.

Gaither LA, Eide DJ. Functional expression of the human hZIP2 zinc transporter. *J Biol Chem.* 2000;275:5560–5564.

Ghatak S, Oliveria P, Kaplan P, Ho SM. Expression and regulation of metallothionein mRNA levels in the prostates of noble rats: lack of expression in the ventral prostate and regulation by sex hormones in the dorsolateral prostate. *Prostate.* 1996;29:91–100.

Gunshin H, Mackenzie B, Berger UV, et al. Cloning and characterization of a mammalian proton-coupled metal-ion transporter. *Nature.* 1997;388:482–487.

Gyorkey F, Min K., Huff JA, Gyorkey P. Zinc and magnesium in human prostate gland: normal, hyperplastic, and neoplastic. *Cancer Res.* 1967;27:1348–1353.

Huang L, Gitschier J. A novel gene involved in zinc transporter is deficient in the lethal milk mouse. *Nat Genet.* 1997;17:292–297.

Huggins C, Hodges CV. Studies on prostatic cancer. I: the effect of castration, of estrogen and of androgen injection on serum phosphatases in metastatic carcinoma of the prostate. *Cancer Res.* 1941;1:293–297.

Iguchi K, Hamatake M, Ishida R, et al. Induction of necrosis by zinc in prostate carcinoma cells and identification of proteins increased in association with this induction. *Eur J Biochem.* 1998;253:766–770.

Ishii K, Usui S, Sugimura Y, Yamamoto H, Yoshikawa K, Hirano K. Inhibition of aminopeptidase N (AP-N) and urokinase-type plasminogen activator (uPA) by zinc suppresses the invasion activity in human urological cancer cells. *Biol Pharm Bull.* 2001;24:226–230.

Kokontis J, Takakura K, Hay N, Liao S. Increased androgen receptor activity and altered c-myc expression in prostate cancer cells after long-term androgen deprivation. *Cancer Res.* 1994;54:1566–1573.

Langmade SJ, Ravindra R, Daniels PJ, Andrews GK. The transcription factor MTF-1 mediates metal regulation of the mouse ZnT1 gene. *J Biol Chem.* 2000;275:34803–34809.

Lee JY, Cole TB, Palmiter RD, Koh JY. Accumulation of zinc in degen-

erating hippocampal neurons of ZnT3-null mice after seizures: evidence against synaptic vesicle origin. *J Neurosci.* 2000;20:RC79 (1–5).

Liang Y, Liu Y, Zou J, Franklin RB, Costello LC, Feng P. Inhibitory effect of zinc on human prostatic carcinoma cell growth. *Prostate.* 1999;40:200–207.

Lowry OH, Rosebrough NJ, Farr AL, Randall RJ. Protein measurement with the folin phenol reagent. *J Biol Chem.* 1951;193:265–275.

Mawson CA, Fischer MI. Zinc content of the genital organs of the rat. *Nature.* 1951;167:859.

Mawson CA, Fischer MI. The occurrence of zinc in the human prostate gland. *Can J Med Sci.* 1952;30:336–339.

Mawson CA, Fischer MI. Zinc and carbonic anhydrase in human semen. *Biochem J.* 1953;55:696–700.

McMahon RJ, Cousins RJ. Regulation of the zinc transporter ZnT-1 by dietary zinc. *Proc Natl Acad Sci U S A.* 1998;95:4841–4846.

Murgia C, Vespognani I, Cerase J, Nobio N, Perozzi G. Cloning, expression, and vesicular localization of zinc transporter Dri 27/ZnT4 in intestinal tissue and cells. *Am J Physiol.* 1999;277:G1231-G1239.

Ogunlewe JO, Osegbe DN. Zinc and cadmium concentrations in indigenous blacks with normal, hypertrophic, and malignant prostate. *Cancer.* 1989;63:1388–1392.

Onishi T, Yamakawa K, Franco OE, Kawamura J, Watanabe M, Shiraishi T, Kitazawa S. Mitogen-activated protein kinase pathway is involved in alpha6 integrin gene expression in androgen-independent prostate cancer cells: role of proximal Sp1 consensus sequence. *Biochim Biophys Acta.* 2001;1538:218–227.

Onishi T, Yamakawa K, Franco OE, Suzuki R, Kawamura J. p27Kip1 is the key mediator of phenylacetate induced cell cycle arrest in human prostate cancer cells. *Anticancer Res.* 2000;20:3075–3081.

Onosaka S, Tanaka K, Doi M, Okahara K. A simplified procedure for determination of metallothionein in animal tissues. *Eisei Kagaku.* 1978;24:128–131.

Pagé B, Pagé M, Noël C. A new fluorometric assay for cytotoxicity measurements *in vitro. Int J Oncol.* 1993;3:473–476.

Palmiter RD. The elusive function of metallothioneins. *Proc Natl Acad Sci U S A.* 1998;95:8428–8430.

Palmiter RD, Cole TB, Findley SD. ZnT-2, a mammalian protein that confers resistance to zinc by facilitating vesicular sequestration. *EMBO J.* 1996a;15:1784–1791.

Palmiter RD, Cole TB, Quaife CJ, Findley SD. ZnT-3, a putative transporter of zinc into synaptic vesicles. *Proc Natl Acad Sci U S A.* 1996b; 93:14934–14939.

Palmiter RD, Findley SD. Cloning and functional characterization of a mammalian zinc transporter that confers resistance to zinc. *EMBO J.* 1995;14:639–649.

Prasad AS. Zinc deficiency in human subjects. *Prog Clin Biol Res.* 1983; 129:1–33.

Prasad AS. Clinical and biochemical manifestation zinc deficiency in human subjects. *J Pharmacol.* 1985;16:344–352.

Shiina H, Igawa M, Ishibe T. Estramustine-binding protein to dihydrotestosterone ratio in human prostatic carcinoma: a new marker for predicting disease progression. *Br J Urol.* 1996a;77:96–101.

Shiina H, Igawa M, Ishibe T. Clinical study on estramustine binding protein (EMBP) in human prostate. *Prostate.* 1996b;29:169–176.

Tohyama C, Suzuki JS, Homma S, Karasawa M, Kuroki T, Nishimura H, Nishimura N. Testosterone-dependent induction of metallothionein in genital organs of male rats. *Biochem J.* 1996;317:97–102.

Yamashita A, Hayashi N, Sugimura Y, Cunha GR, Kawamura J. Influence of diethylstilbestrol, Leuprolelin (a luteinizing hormone-releasing hormone analog), Finasteride (a 5 α-reductase inhibitor), and castration on the lobar subdivisions of the rat prostate. *Prostate.* 1996;29:1–14.

Journal of Andrology, Vol. 23, No. 6, November/December 2002
Copyright © American Society of Andrology

High-Level Expression of Zinc Transporter-2 in the Rat Lateral and Dorsal Prostate

KAZUHIRO IGUCHI,* SHIGEYUKI USUI,* TAKAHIRO INOUE,† YOSHIKI SUGIMURA,‡ MASAE TATEMATSU,§ AND KAZUYUKI HIRANO*

*From the *Laboratory of Pharmaceutics, Gifu Pharmaceutical University, Mitahora-higashi, Gifu, Japan; †Department of Urology, Kyoto University Graduate School of Medicine, Shogoin, Kawara-cho, Sakyo-ku, Kyoto, Japan; ‡Department of Urology, Mie University School of Medicine, Edobashi, Tsu, Mie, Japan; and §Department of Tumor Pathology, Aichi Cancer Center Hospital, Kanokoden, Chikusa-ku, Nagoya, Japan.*

ABSTRACT: Zinc is present at high concentrations in the prostate gland, however, the zinc-retention system in the prostate remains obscure. In this study, we investigated the expression of zinc transporters in the rat prostate and found that zinc transporter-2 (ZnT2), which sequesters zinc to the lysosome-like compartment, is expressed at high levels in the lateral prostate (LP) and dorsal prostate (DP), and that these areas contain higher levels of zinc than other tissues such as the ventral prostate (VP), liver, and kidney. Zinc levels in LP from castrated rats were lower than those in sham-operated rats. However, expression of ZnT2 in LP and DP was unaffected by castration. Expression of other zinc transporters (ZnT1, ZnT4, and divalent cation transporter 1) did not correlate with zinc levels. These results suggest that factors that regulate zinc homeostasis other than zinc transporters are involved in lowering zinc content after castration in rat prostate.

Key words: Castration, lysosome, zinc.

J Androl 2002;23:819–824

High concentrations of zinc, an essential trace element for most cells, are known to be retained in the prostate gland and secreted into the seminal plasma (Mawson and Fischer, 1951, 1952, 1953). Zinc is required for maintenance and activity of numerous metalloproteins, where it plays either a structural role or it has a catalytic function as part of the active sites of various metalloenzymes (Prasad, 1995; McCall et al, 2000). Zinc has also been suggested to have an antibacterial function in seminal plasma (Fair et al, 1976) and to be essential for optimal development and maintenance of the male reproductive system (Favier, 1992; Nishi, 1996). Recently, zinc was reported to control prostatic epithelial cell growth by inhibiting mitochondrial aconitase activities, cell cycle arrest, and induction of cell detachment (Costello and Franklin, 1981; Costello et al, 1997; Iguchi et al, 1998; Liang et al, 1999). Although the physiological functions of zinc in the prostate have been gradually revealed, the reason why zinc accumulates in the prostate remains unclear.

Many transporters that regulate zinc homeostasis have been identified in mammals. Divalent cation transporter 1 (DCT1) is a metal ion transporter that imports a variety of metal ions such as iron, zinc, cadmium, and copper from the extracellular environment into cells (Gunshin et al, 1997). Zinc transporter 1 (ZnT1), which was found by Palmiter et al (1996) using zinc-sensitive BHK cells, exports zinc out of cells to prevent zinc toxicity (Palmiter and Findley, 1995). ZnT2 is involved in zinc uptake into vesicles (endosome/lysosome compartment) in the intestine, kidney, and testis (Palmiter et al, 1996). ZnT4, which was identified using the positional cloning method, is also involved in zinc uptake into vesicles in the mammary gland, and was identified as the molecular basis of the recessive mouse mutation, "lethal milk syndrome" (Huang and Gitschier, 1997; Murgia et al, 1999). DCT1, ZnT1, and ZnT4 are ubiquitously expressed in most tissues, whereas ZnT2 displays tissue-restricted expression in rats.

The rat prostate consists of at least three anatomically independent lobes, designated as the ventral (VP), lateral (LP), and dorsal (DP) prostates. Biochemical compositions have been compared among these prostates. For example, VP was reported to secrete mainly citrate, polyamines, and spermine (Gerhardt et al, 1983). LP and DP were known to retain high levels of zinc in their lumen and epithelial cells (Chandler et al, 1977a,b; Sorensen et al, 1997). Moreover, the level of zinc was shown to decrease in LP, but to increase in VP following castration (Timms and Chandler, 1983; Yamashita et al, 1996; Liu et al, 1997). Although the level of zinc in the prostate is hormonally controlled, the mechanisms resulting in the above differences and the differential hormonal responsiveness among these lobes remain obscure.

Correspondence to: Dr Kazuyuki Hirano, Laboratory of Pharmaceutics, Gifu Pharmaceutical University, 5-6-1 Mitahora-higashi, Gifu 502-8585, Japan (e-mail: hirano@gifu-pu.ac.jp).

Received for publication May 23, 2002; accepted for publication February 4, 2002.

Possible relationships between changes in zinc content in the prostate and prostatic diseases have been vigorously investigated. Zinc concentrations in the prostate gland were reported to be significantly lower in patients with prostatic cancer, and higher in those with benign prostatic hyperplasia, compared with levels in normal glands (Gyorkey et al, 1967; Ogunlewe and Osegbe, 1989). Zinc levels in seminal plasma of patients with bacterial prostatitis or sterility were observed to be consistently lower than those in healthy subjects (Fair et al, 1976; Nishi, 1996). Although functional disorder of zinc homeostasis seems to be associated with prostatic disease, it is unclear whether diseases cause the disruption of zinc homeostasis or vice versa.

In the present study, expression of zinc transporters in the rat prostate was examined by semiquantitative reverse transcription-polymerase chain reaction (RT-PCR) to clarify whether a zinc retention system by these transporters exists in the prostate. Elucidation of the zinc retention system in the prostate will be useful for investigating prostatic diseases.

Experimental Procedure

Animal Protocols

Animal protocols were approved by the Animal Care and Use Committee of Gifu Pharmaceutical University. Male Sprague-Dawley rats, 12 weeks old, were housed in an environmentally controlled room (25°C, 12 L:12 D cycle) and fed standard chow pellets and water ad libitum. Castration was performed surgically under Nembutal anesthetization via the scrotal route. Castrated and sham-operated rats were killed at 14 days postcastration and tissues were collected. The tissues were rapidly removed after rats were killed, and stored at −80°C until use.

Semiquantitative RT-PCR

Total cellular RNA was isolated using TRIzol reagent (Life Technologies, Inc, Rockville, Md) according to the manufacturer's instructions. Extracted RNA was dissolved in diethylpyrocarbonate (DEPC)-treated water and quantified by measuring the absorbance at 260 nm. Aliquots of 5 μg of total RNA were used to synthesize the first-strand complementary DNA (cDNA) with SuperScript II (Life Technologies) and subjected to PCR amplification with the oligonucleotide primers listed in Table 1 using a thermal cycler. The optimal PCR conditions were determined as the amount of amplification product in proportion to that of input RNA. PCR was performed under the following conditions: 26 cycles for 1 minute at 94°C, 1 minute at 57°C, and 1 minute at 72°C for ZnT1, ZnT2, and ZnT4; 27 cycles for 1 minute at 94°C, 1 minute at 59°C, and 1 minute at 72°C for DCT1; 24 cycles for 1 minute at 94°C, 1 minute at 58°C, and 1 minute at 72°C for glyceraldehyde-3-phosphate dehydrogenase (G3PDH). Control reactions for RT-PCR were performed by replacing the RNA sample with DEPC-treated water. G3PDH served as an internal RNA control to allow comparison of RNA levels among different specimens. After PCR, the reaction products were resolved on 1.75% agarose gels and visualized with ethidium bromide.

Table 1. *Sequences of oligonucleotide primers for PCR*

Zinc Transporter	Primer	Size of Amplified Product (base pairs)
ZnT1		
5′-Primer	5′-GGAGTGGAGGAAGTCCATGA-3′	897
3′-Primer	5′-GGCACGTAACTACCCCTCAA-3′	
ZnT2		
5′-Primer	5′-TCCATCAGTCTGGACATGGA-3′	266
3′-Primer	5′-CCCTTCCATGAGAACCAAGA-3′	
ZnT4		
5′-Primer	5′-ACCTTGCAGCAGGACCTAGA-3′	301
3′-Primer	5′-ATACTGCCGTGGAGAAATGC-3′	
DCT1		
5′-Primer	5′-GCCCCAGAGTTCTGCTGTAG-3′	263
3′-Primer	5′-GCAGAAGAACGAGGACCAAG-3′	
G3PDH*		
5′-Primer	5′-ATGACTCTACCCACGGCAAG-3′	388
3′-Primer	5′-ACTGTGGTCATGAGCCCTTC-3′	

* Used as an internal RNA control.

Tissue Preparation

Rat tissues were dissected and immediately frozen in liquid nitrogen to extract RNA. For other procedures, tissues were fractionated as described previously (Rowin, 1974; Compton and Witorsch, 1984). Briefly, tissues were pulverized, placed in 7 volumes of 0.25 M sucrose, and homogenized. The homogenate was centrifuged at 600 × *g* for 10 minutes and the resulting supernatant was then centrifuged at 3300 × *g* for 10 minutes. The precipitate obtained was resuspended in 0.25 M sucrose and designated as the heavy mitochondrial fraction. The supernatant was subsequently centrifuged at 25 000 × *g* for 10 minutes to obtain the pellet. This pellet was resuspended in 0.25 M sucrose and designated as the light mitochondrial fraction, which contained lysosomes. The resulting supernatant was further centrifuged at 100 000 × *g* for 60 minutes and the supernatant obtained was considered the cytosol. These fractions were used to determine the contents of zinc and the activity of acid phosphatase. For zinc assay with whole tissue, the samples were prepared using 7 volumes of Milli-Q water (Millipore Corp, Bedford, Mass) instead of 0.25 M sucrose. Protein concentrations were determined by the Bradford assay (Bradford, 1976) using bovine serum albumin as a standard.

Zinc Assay

Zinc was assayed by atomic absorption as described previously (Liu et al, 1997), after samples were digested in trichloroacetic acid/nitric acid (50/50) solution in a boiling water bath for 30 minutes.

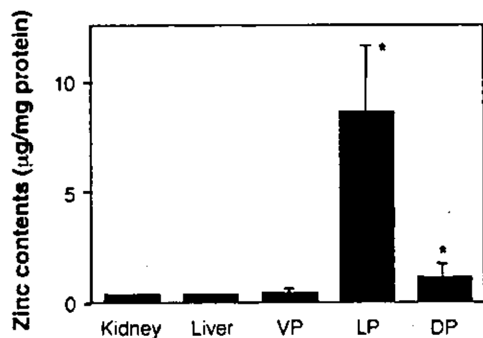

Figure 1. Zinc levels in different tissues of normal rats. Total zinc levels of tissues were determined as described in "Experimental Procedure." Values are expressed as means ± SD of 8 animals. *$P < .05$ versus values obtained in kidney.

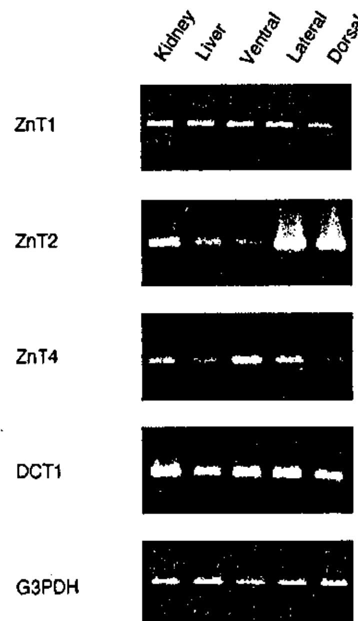

Figure 2. RT-PCR analysis of zinc transporter mRNA expression in rat tissues. Total RNA was purified from rat tissues and subjected to RT-PCR. The products were resolved on 1.75% agarose gels and visualized with ethidium bromide. Data shown are representative of at least 3 animals.

Acid Phosphatase Activity

Acid phosphatase activity was assayed according to the method described by Kind and King (1954) and expressed as King-Armstrong units per milligram of protein.

Statistical Analysis

The significance of differences between groups was calculated using the Student *t*-test.

Results

Expression of Zinc Transporters in Rat Tissues

Zinc levels in the prostate and other tissues are presented in Figure 1. The results demonstrated that zinc levels in LP and DP were approximately 30-fold and 4-fold higher, respectively, than those in other tissues. The zinc level in VP was nearly the same as levels in kidney and liver (Figure 1).

To determine what kinds of transporters are involved in the zinc transport system in the rat prostate gland, expression levels of zinc transporters were examined by semiquantitative RT-PCR. ZnT1, ZnT2, ZnT4, and DCT1 were chosen as candidates of the transporters because expression of these factors has been identified in rats. As shown in Figure 2, ZnT2 messenger RNA (mRNA) was expressed at higher levels in LP and DP than it was in other tissues, and ZnT4 mRNA expression in VP was found to be highest in three anatomically independent lobes of the prostate. The sample RNAs that had not been reverse-transcribed did not yield a PCR product (data not shown).

Because ZnT2 is known to transport zinc into lysosomes (Palmiter et al, 1996), zinc is expected to accumulate in lysosomes of LP and DP in which ZnT2 was observed to be expressed at high levels. Therefore, zinc amounts, together with those of acid phosphatase, which is considered a lysosomal marker enzyme, were determined after subcellular fractionation of tissues. As shown in Table 2, acid phosphatase activity was predominantly detected in the light mitochondrial fractions of all tissues listed and was lowest in all cytosolic fractions among the three subcellular fractions, except that the activity in the subcellular fractions of LP was quite low. This low activity may have been due to the inhibitory effects of high levels of zinc in LP as described below, because zinc ions

Table 2. *Acid phosphatase activity in subcellular fractions of various rat tissues*[a]

(King-Armstrong units/mg protein)	Kidney	Liver	VP	LP	DP
3.3 k × g pellet	14.4 ± 0.5[b]	8.7 ± 0.9	19.5 ± 4.2[b]	8.1 ± 2.4	24.7 ± 6.0[b]
25 k × g pellet	21.7 ± 1.4[b]	15.7 ± 0.9[b]	27.0 ± 9.8[b]	6.6 ± 1.7	45.6 ± 9.3[b]
100 k × g supernatant	11.0 ± 1.1	8.6 ± 1.1	5.3 ± 0.6	7.2 ± 1.4	8.6 ± 1.9

[a] Acid phosphatase activity is expressed as King-Armstrong units per milligram of protein. Values are expressed as means ± SD of 10–15 animals.
[b] $P < .01$ versus values obtained in 100 k × g supernatant fractions of each tissue.

Table 3. *Subcellular distribution of zinc in rat tissues*[a]

ng zinc/mg protein	Kidney	Liver	VP	LP	DP
3.3 k × g pellet	152 ± 20[b]	166 ± 11[b]	320 ± 138	12149 ± 3686	2992 ± 1287[b]
25 k × g pellet	179 ± 22[b]	204 ± 30[b]	332 ± 135	19019 ± 591	3244 ± 1954[b]
100 k × g supernatant	313 ± 55	295 ± 32	207 ± 101	15524 ± 6416	1013 ± 427

[a] Values are expressed as means ± SD of 10–15 animals.
[b] $P < .001$ versus values obtained in 100 k × g supernatant fractions of each tissue.

are known to inhibit the activity of acid phosphatase (DeChatelet et al, 1971). Thus, the fractionation was judged to be sufficient. As shown in Table 3, DP zinc levels in the heavy mitochondrial fraction and the light mitochondrial fraction, which contained lysosomes, were about threefold higher than that in the cytosolic fraction. The zinc level in the light mitochondrial fraction from LP was slightly higher than it was in the heavy mitochondrial and cytosolic fractions, but the differences were not significant. This probably represents the contamination of the cytosolic fraction in LP with zinc from the lumen, because our method was unable to separate zinc from the epithelial cells and lumen. On the other hand, zinc levels in the light mitochondrial fraction from VP, liver, and kidney were no higher than those in the heavy mitochondrial and cytosolic fractions.

Expression of Zinc Transporters in Castrated Rat Tissues

Zinc levels in various tissues from castrated and sham-operated rats are presented in Table 4. The level of zinc in LP from castrated rats was significantly lower than it was in sham-operated rats. On the other hand, zinc levels in VP of castrated rats was twofold higher than it was in sham-operated rats. No significant differences in zinc content of the other tissues were observed after castration.

Because hormone manipulation is known to regulate the zinc level in the prostate, expression levels of zinc transporters in castrated and sham-operated rats were investigated. As shown in Figure 3, although ZnT2 mRNA expression in LP was not affected by castration, its expression in VP was slightly increased. Messenger RNA expression of the other transporters examined was unaffected by castration.

Discussion

In the present study, we demonstrated that high levels of ZnT2 mRNA were expressed in LP and DP, and we also showed that the lysosome-rich subcellular fraction contained a higher concentration of zinc than the other fractions. ZnT2 has been reported to be localized in the lysosomes and to sequester zinc into the vesicular compartments based on the observation of colocalization of ZnT2/green fluorescent fusion protein with LysoTracker (Molecular Probes, Eugene, Ore) and acridine orange, endosomal/lysosomal fluorescent dyes (Palmiter et al, 1996). Moreover, the lysosome-like compartment in rat LP was shown to contain a high level of zinc by x-ray microanalysis (Chandler et al, 1977a,b; Sorensen et al, 1997). These observations and our results indicate that ZnT2 in LP and DP sequesters intracellular zinc to the lysosome-like compartment.

Accumulation of zinc in the prostate has been reported to be regulated by hormones in vivo and in vitro. Animal experiments showed that administration of testosterone and prolactin raised zinc levels in LP, and lowered them in VP. In contrast, our results (shown in Table 4) and previous reports showed that castration lowered zinc levels in LP and raised them in VP (Timms and Chandler, 1983; Yamashita et al, 1996; Liu et al, 1997). Moreover, in vitro studies have revealed that testosterone and prolactin regulate the zinc transport system in human prostatic LNCaP and PC-3 cells (Costello et al, 1999). From these observations, we first suspected that ZnT2, which is highly expressed in LP and DP, was under hormonal control. In the present study, however, with androgen ablation, no significant changes in ZnT2 mRNA expression were observed in LP or DP, where most zinc is present,

Table 4. *Effect of castration on zinc contents in rat tissues*[a]

ng zinc/ mg protein	Kidney	Liver	VP	LP	DP
Sham	278 ± 43	265 ± 22	262 ± 96	9436 ± 2952	1231 ± 606
Castration	236 ± 55	221 ± 28	432 ± 104[b]	2222 ± 1253[b]	1040 ± 728

[a] Values are expressed as means ± SD of six individual animals.
[b] $P < .01$ versus values obtained in sham operation.

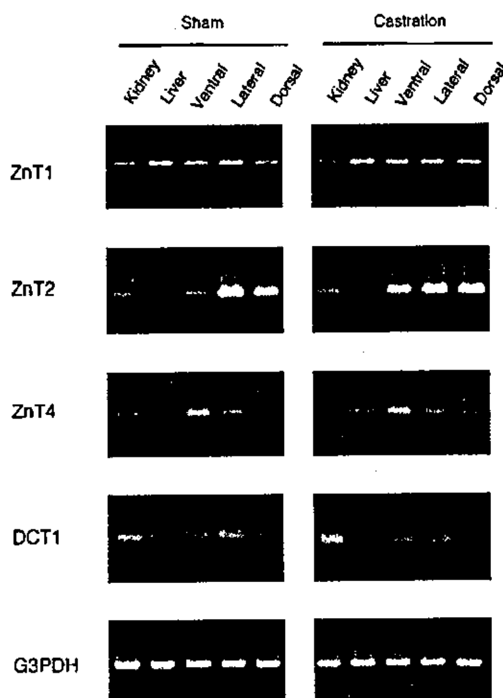

Figure 3. Effect of castration on mRNA expression of zinc transporters. Total RNA was purified from castrated and sham-operated rat tissues. Messenger RNA expression of zinc transporters was examined with semiquantitative RT-PCR. The products were resolved on 1.75% agarose gels and visualized with ethidium bromide. Data shown are representative for at least 3 animals.

although zinc levels were lower in the prostate. Therefore, ZnT2 expression would not be involved in the decrease of zinc levels in the prostate of castrated rats.

Although ZnT2 expression in LP and DP was not changed by castration, a significant increase in its mRNA expression was observed in VP. The number of epithelial cells is known to be significantly lowered by castration in VP compared with those in LP and DP (Kiplesund et al, 1988). If the difference in ZnT2 expression levels is found between epithelial cells and stromal cells, the shift in the cellular ratio by castration may affect the change in ZnT2 mRNA expression observed in VP. Moreover, because the androgen receptor was reported to be abundantly expressed in VP compared with LP and DP (Prins, 1989), then VP is generally more susceptible to hormones than the other parts of prostate and requires androgens for its morphological and functional maintenance. The expression of ZnT2 mRNA in VP may be at least in part inhibited by androgens.

We also found that higher levels of ZnT4 mRNA were expressed in VP than in LP and DP. ZnT4 is known to be localized in the membrane of intracellular vesicles and to sequester zinc into the vesicular compartments (Murgia et al, 1999). A single point mutation in ZnT4 was demonstrated to result in lethal milk syndrome (Huang and Gitschier, 1997). The milk produced by homozygous ZnT4 mutant females contains insufficient zinc to support the needs of growing mice pups. ZnT4 in VP might be involved in the secretory role of zinc into the seminal plasma in a manner similar to ZnT4 in the mammary gland, where ZnT4 is presumed to secrete zinc into the milk. Lower levels of zinc in seminal plasma were found in patients with prostatitis or sterility (Fair et al, 1976; Nishi, 1996). ZnT4 expression levels in these patients are expected to be determined in future studies.

In this study, high levels of zinc were observed in not only the light mitochondrial fraction, which contains lysosomes, but also in the heavy mitochondrial fraction in DP. Franklin et al demonstrated that accumulation of high levels of zinc in the mitochondria of prostate cells inhibited mitochondrial aconitase activity (Costello and Franklin, 1981; Costello et al, 1997). Inhibition of aconitase activity, which regulates ATP production, suppressed the growth of prostatic epithelial cells. Thus, the role of mitochondrial zinc in the prostate is being clarified. On the other hand, no information is available at present concerning the high levels of zinc in lysosomes and its regulation in the prostate. Zinc in lysosomes is known to mediate stabilization of the lysosomal membrane (Chvapil et al, 1972), to modify various enzyme activities (DeChatelet et al, 1971; Shin and Mego, 1988; Hiraiwa et al, 1993), and to modify intracellular cholesterol transport (Kobayashi et al, 1999). These functions may affect the roles of zinc in the lysosomes in the prostate.

Zinc levels in VP were nearly the same as those in the kidney and liver (Figure 1), whereas Liu et al (1997) reported that zinc levels in VP were approximately threefold higher than those in the kidney and liver. This discrepancy might be explained by contamination by serum zinc because liver and kidney perfusion were not carried out in our experiments.

In conclusion, this is the first report of the observation of ZnT2 mRNA in rat LP and DP. In addition, no androgenic regulation of ZnT2 mRNA was found in LP or DP. Changes in zinc concentration in prostatic diseases have been well defined. Although ZnT2 expression was suggested to be unrelated to changes in zinc levels in the prostate of castrated rats, clarification of the relationship between ZnT2 expression and prostatic diseases might help in understanding the physiology of the prostate.

References

Bradford MM. A rapid and sensitive method for the quantitation of microgram quantities of protein utilizing the principle of protein-dye binding. *Anal Biochem.* 1976;72:248–254.

Chandler JA, Sinowatz F, Timms BG, Pierrepoint CG. The subcellular

distribution of zinc in dog prostate studied by x-ray microanalysis. *Cell Tissue Res.* 1977a;185:89–103.

Chandler JA, Timms BG, Morton MS. Subcellular distribution of zinc in rat prostate studied by x-ray microanalysis: I. Normal prostate. *Histochem J.* 1977b;9:103–120.

Chvapil M, Ryan JN, Zukoski CF. The effect of zinc and other metals on the stability of lysosome. *Proc Soc Exp Biol Med.* 1972;140:642–646.

Compton MM, Witorsch RJ. Proteolytic degradation and modification of rat prolactin by subcellular fractions of the rat ventral prostate gland. *Endocrinology.* 1984;115:476–484.

Costello LC, Franklin RB. Aconitase activity, citrate oxidation, and zinc inhibition in rat ventral prostate. *Enzyme.* 1981;26:281–287.

Costello LC, Liu Y, Zou J, Franklin RB. Evidence for a zinc uptake transporter in human prostate cancer cells which is regulated by prolactin and testosterone. *J Biol Chem.* 1999;274:17499–17504.

Costello LC, Liu Y, Franklin RB, Kennedy MC. Zinc inhibition of mitochondrial aconitase and its importance in citrate metabolism of prostate epithelial cells. *J Biol Chem.* 1997;272:28875–28881.

DeChatelet LR, Cooper MR, McCall CE. Studies on leukocyte phosphatases. 3. Inhibition of leukocyte acid phosphatase by zinc. *Clin Chem.* 1971;17:1176–1179.

Fair WR, Couch J, Wehner N. Prostatic antibacterial factor. *Urology.* 1976;7:169–177.

Favier AE. The role of zinc in reproduction. Hormonal mechanisms. *Biol Trace Elem Res.* 1992;32:363–382.

Gerhardt PG, Mevag B, Tveter KJ, Purvis K. A systematic study of biochemical differences between the lobes of the rat prostate. *Int J Androl.* 1983;6:553–562.

Gunshin H, Mackenzie B, Berger UV, et al. Cloning and characterization of a mammalian proton-coupled metal-ion transporter. *Nature.* 1997; 388:482–487.

Gyorkey F, Min K, Huff JA, Gyorkey P. Zinc and magnesium in human prostate gland: normal, hyperplastic, and neoplastic. *Cancer Res.* 1967;27:1348–1353.

Hiraiwa M, Yamauchi T, Tsuji S, Nishizawa M, Miyatake T, Oyanagi K, Ikuta F, Uda Y. Activation of human lysosomal sialidase. *J Biochem.* 1993;114:901–905.

Huang L, Gitschier J. A novel gene involved in zinc transport is deficient in the lethal milk mouse. *Nat Genet.* 1997;17:292–297.

Iguchi K, Hamatake M, Ishida R, et al. Induction of necrosis by zinc in prostate carcinoma cells and identification of proteins increased in association with this induction. *Eur J Biochem.* 1998;253:766–770.

Kind PRN, King EJ. Estimation of plasma phosphatase by determination of hydrolyzed phenol with aminoantipyrine. *J Clin Pathol.* 1954;7: 332–336.

Kiplesund KM, Halgunset J, Fjosne HE, Sunde A. Light microscopic morphometric analysis of castration effects in the different lobes of the rat prostate. *Prostate.* 1988;13:221–232.

Kobayashi T, Beuchat MH, Lindsay M, Farias S, Palmiter RD, Sakuraba H, Parton RG, Gruenberg J. Late endosomal membranes rich in lysobisphosphatidic acid regulate cholesterol transport. *Nat Cell Biol.* 1999;1:113–118.

Liang Y, Liu Y, Zou J, Franklin RB, Costello LC, Feng P. Inhibitory effect of zinc on human prostatic carcinoma cell growth. *Prostate.* 1999;40:200–207.

Liu Y, Franklin RB, Costello LC. Prolactin and testosterone regulation of mitochondrial zinc in prostate epithelial cells. *Prostate.* 1997;30:26–32.

Mawson CA, Fischer MI. Zinc content of the genital organs of the rat. *Nature.* 1951;167:859.

Mawson CA, Fischer MI. The occurrence of zinc in the human prostate gland. *Can J Med Sci.* 1952;30:336–339.

Mawson CA, Fischer MI. Zinc and carbonic anhydrase in human semen. *Biochem J.* 1953;55:696–700.

McCall KA, Huang C-C, Fierke CA. Function and mechanism of zinc metalloenzymes. *J Nutr.* 2000;130:1437S–1446S.

Murgia C, Vespognani I, Cerase J, Nobio N, Perozzi G. Cloning, expression, and vesicular localization of zinc transporter Dri 27/ZnT4 in intestinal tissue and cells. *Am J Physiol.* 1999;277:G1231–G1239.

Nishi Y. Zinc and growth. *J Am Coll Nutr.* 1996;15:340–344.

Ogunlewe JO, Osegbe DN. Zinc and cadmium concentrations in indigenous blacks with normal, hypertrophic, and malignant prostate. *Cancer.* 1989;63:1388–1392.

Palmiter RD, Cole TB, Findley SD. ZnT-2, a mammalian protein that confers resistance to zinc by facilitating vesicular sequestration. *EMBO J.* 1996;15:1784–1791.

Palmiter RD, Findley SD. Cloning and functional characterization of a mammalian zinc transporter that confers resistance to zinc. *EMBO J.* 1995;14:639–649.

Prasad AS. Zinc: an overview. *Nutrition.* 1995;11:93–99.

Prins GS. Differential regulation of androgen receptors in the separate rat prostate lobes: androgen independent expression in the lateral lobe. *J Steroid Biochem.* 1989;33:319–326.

Rowin GL. Isolation of lysosomes. In: Laskin AI, Last JA, eds. *Subcellular Particles, Structures and Organelles.* New York: Marcel-Dekker; 1974:89–109.

Shin HJ, Mego JL. A rat liver lysosomal membrane flavin-adenine dinucleotide phosphohydrolase: purification and characterization. *Arch Biochem Biophys.* 1988;267:95–103.

Sorensen MB, Stoltenberg M, Juhl S, Danscher G, Ernst E. Ultrastructural localization of zinc ion in the rat prostate: an autometallographic study. *Prostate.* 1997;31:125–130.

Timms BG, Chandler KA. Effects of androgens on the ultrastructure and subcellular zinc distribution in the prostatic epithelium of castrated rats. *Prostate.* 1983;4:57–72.

Yamashita A, Hayashi N, Sugimura Y, Cunha GR, Kawamura J. Influence of diethylstilbestrol, Leuprolelin (a luteinizing hormone-releasing hormone analog), Finasteride (a 5α-reductase inhibitor), and castration on the lobar subdivisions of the rat prostate. *Prostate* 1996;29:1–14.

Environmental Health Perspectives 103, Supplement 7, October 1995

Effects of Sex Hormones on Oncogene Expression in the Vagina and on Development of Sexual Dimorphism of the Pelvis and Anococcygeus Muscle in the Mouse

Taisen Iguchi,[1] Yugo Fukazawa,[1] and Howard A. Bern[2]

[1]Department of Biology, Yokohama City University, Yokohama, Japan;
□[2]Department of Integrative Biology and Cancer Research Laboratory,
University of California, Berkeley, California

Abstract

Neonatal treatment of female mice with diethylstilbestrol (DES) is known to induce ovary-independent persistent proliferation and cornification of vaginal epithelium. This irreversibly changed vaginal epithelium persistently expressed higher levels of c-*jun* and c-*fos* mRNAs, which was not altered by postpubertal estrogen. Sexual dimorphism was encountered in mouse pelvis and anococcygeus muscle. Postpubertal estrogen changed the shape of the pelvis to the female type and postpubertal androgen changed it to the male type. Neonatal exposure to DES and to the antiestrogen tamoxifen altered the developmental pattern of the pelvis, which contained lower concentrations of calcium and phosphorus than controls. The size of anococcygeus muscle was increased by postpubertal androgen but decreased by postpubertal estrogen. However, neonatal estrogen (DES) exposure permanently enlarged the anococcygeus muscle. Thus neonatal treatment of mice with estrogen and antiestrogen results

in irreversible changes in nonreproductive as well as reproductive structures. --
Environ Health Perspect 103(Suppl 7):79-82 (1995)
Key words: developmental effects, diethylstilbestrol, tamoxifen, vagina, oncogene expression, sexual dimorphism, pelvis, anococcygeus muscle, estrogen receptor

This paper was presented at the Symposium on Estrogens in the Environment, III: Global Health Implications held 9-11 January 1994 in Washington, DC. Manuscript received: March 15, 1995; manuscript accepted: April 4, 1995.

This work was supported by a Grant-in-Aid for Scientific Research from the Ministry of Education, Science, and Culture of Japan, a research grant from Kihara Science Foundation, a grant in Support of the Promotion of Research at Yokohama City University, and funds from Zenyaku Kogyo Company of Tokyo.

Address correspondence to Dr. Taisen Iguchi, Department of Biology, Yokohama City University, 22-2 Seto, Kanazawa-Ku, Yokohama 236, Japan. Telephone 81 45 787 2216. Fax 81 45 787 2316.

Introduction

The study of permanent changes in target organs induced by sex hormones administered during a critical period of development began with experiments on the neonatal mouse treated with estrogens (*1-4*). The vaginal epithelium of mice treated neonatally with estrogen, including diethylstilbestrol (DES), showed persistent proliferation and cornification, frequently resulting in precancerous and cancerous lesions (*5*). Perinatally sex hormone-exposed female rodents show lesions in vagina and cervix, uterine metaplasia and tumors, oviducal malformations and tumors, polyovular follicles in the ovary, and mammary gland hyperplasia, dysplasia, and neoplasia (*6-12*). Perinatal treatment of male mice

with estrogenic hormones gives rise to neoplastic changes in coagulating gland, seminal vesicle, and testis (*13,14*). Nongenital abnormalities have also been reported in mice exposed perinatally to sex hormones and antihormones (*12,15-18*). This paper describes briefly some genital and nongenital abnormalities found in mice exposed neonatally to the estrogen DES and to the antiestrogen tamoxifen.

Proto-oncogene Expression in Vagina and Uterus of Mice Exposed Neonatally to DES

Estrogens stimulate DNA synthesis and cell proliferation in the female reproductive tract (*19*) by initially binding to high-affinity nuclear estrogen receptors that directly regulate transcription of target genes by binding to DNA estrogen-responsive elements (*20*). Products of the genes activated through the estrogen receptor play a role in amplifying the tissue response. As a primary response to the estrogen receptor complex, c-*fos*, c-*jun* and c-*myc* proto-oncogenes are expressed in immature and adult rat uterus (*21*) and mouse vagina (*22*).

The direct effect of estrogen on the expression of these proto-oncogenes was examined by Northern blot analysis of vagina and uterus in 50-day-old ovariectomized mice exposed neonatally to DES. In ovariectomized, unexposed control mice, the expression of c-*jun* and c-*fos* mRNAs in the uterus was stimulated by 17ß-estradiol. Within 1 hr after estradiol administration at 50 days, c-*jun* and c-*fos* mRNAs increased in concentration, showing a peak 3 hr after estradiol stimulation and decreasing with time thereafter. In the vagina, the concentration of c-*jun* and c-*fos* mRNAs increased rapidly, reaching a peak within 1 hr. The expression of c-*myc* in uterus and vagina was not changed by postpubertal estrogen. Expressions of c-*jun* and c-*fos* mRNAs were greater in both the uterus (3- and 6-fold, respectively) and the vagina (18- and 4-fold) of neonatally DES-exposed mice than in control organs. These increased levels of c-*jun* and c-*fos* expression were not further altered by postpubertal estradiol and may be related to ovary-independent persistent changes in the genital tract.

Mouse Pelvis: Sexual Dimorphism and Responsiveness to Steroid Hormones

The mouse pelvis is sexually dimorphic (*23, 24*). A pair of innominate bones, the ossa coxae, are composed of four separate units: ilium, ischium, pubis, and acetabulum, which unite at the ventral midline as the pubic symphysis to form the pelvis. The innominate bone is connected dorsomedially with the sacrum by the iliosacral joint. Gardner (*23*) reported that there is no difference in the shape of the innominate bone in young male and female mice; however, after sexual maturity, the pubic bone in females is thinner than in males. Long-term administration of estrogenic hormones to male mice induces a female-type pelvis with thin pubic bones, indicating that sex hormones play a role in pelvic morphogenesis.

Sexual dimorphism of the innominate bone was found in adult T-strain rats and Chinese hamsters, as well as in mice, by computer-aided morphometric analysis (*25*). Sexual differences in the pubis and the ischium appeared in mice at 30 and 120 days of age, respectively (*24, 26*). The pubis in female mice was longer and thinner than in males, and the ischium in male mice was shorter and thicker than in females in 14 strains of mice. Serum androgen levels in male mice increased from 30 to 50 days of age (*27*), suggesting that in male mice the shape of pelvic bones is determined by postpubertally secreted androgens.

The ratio of the width of the ischium to the longitudinal length of the innominate bone in 120-day-old female mice was significantly lower than in 30-day-old females; thus ovarian estrogen secreted postpubertally may participate in the formation of the female pelvic bones. In both male and female newborn mice, estrogen receptors were immunohistochemically detected in mesenchymal cells surrounding pubis and ischium and in the periosteum and osteocytes of pubis and ischium, but not in the innominate bone. A weak reaction for the receptors was also observed in the chondrocytes of pubis and ischium (*26*).

The innominate bones from male mice castrated on the day of birth and from female mice given daily injections of 20 μg testosterone and

5-dihydrotestosterone for 5 days starting on the day of birth were examined at 30 days of age. The ratio of the pubis width to innominate length in neonatally androgen-treated females at 30 days was greater than in the age-matched untreated females, whereas this ratio was smaller in neonatally castrated 30-day-old males than in age-matched intact males. In adult testicular-feminized male mice lacking androgen receptors, ischium length and width were significantly smaller than in the wild-type males. Pubis width in testicular-feminized male mice was intermediate between those of wild-type males and females. The ischium in females and castrated males was shorter and thinner than in the males. The pubis in gonadectomized males and females was wider than in intact females and smaller than in intact males. The pubis in intact males and castrated males was shorter than in intact females (*26*).

In summary, the basic type of ischium is the female type; postnatal endogenous androgen modifies the ischium to the male phenotype, and the pubis phenotype is intermediate between males and females; postnatal endogenous androgen induces the male type, and postpubertal endogenous estrogen induces the female type. These results suggest that the shape of the innominate bone is transformed to the male type under the influence of early postnatal androgen (*12,26*).

Neonatal tamoxifen treatment caused a long-lasting inhibition of pubic bone calcification; the elastic and cartilaginous nature of the symphysis region continued into adulthood. Neonatally tamoxifen-exposed mice showed hernia of the urinary bladder with or without descent of the caecum through the subpubic space (*15, 16*). Although the mechanism of the bladder hernia is unknown, it may be related to the modified symphysis pubis. Mice treated with tamoxifen for 5 days starting at 0 to 10 days of age had significantly longer pubic ligaments than did the corresponding controls. However, mice treated neonatally with clomiphene and nafoxidine possessed normal pubic bones (*16*).

In 120-day-old female mice treated neonatally with 100 µg tamoxifen, the total area of the pelvis and the individual areas of the ilium, ischium, and pubis were significantly smaller than in the controls. There was no significant difference in

the length of ischium between tamoxifen-treated and control mice of both sexes. However, lengths of ilium and pubis and widths of ilium, pubis, and ischium in tamoxifen-treated male and female mice were significantly smaller than in the respective controls. In contrast, neonatal treatment with 2 µg DES for 5 days from the day of birth did not affect the shape of the pelvis of either sex (*24*).

Indicators of bone resorption in the endosteal area of the pubic bone were measured on histological sections. The number of active osteoclasts was counted per unit area of bone section. In 15-day-old mice given neonatal injections of tamoxifen, the osteoclastic surface, the number of osteoclasts per unit area, and the number of nuclei per osteoclast were significantly smaller than in the controls. Inhibition of ossification persisted in the junction of pubis and ischium of pelvis transplanted under the kidney capsule after treatment with tamoxifen *in vitro* (*18*).

These findings indicate that neonatally injected tamoxifen mainly retards the growth of the ilium and pubis in mice by changing the activities of osteoclasts and osteoblasts and that tamoxifen acts directly on the neonatal mouse pubis as an antiestrogen to inhibit its ossification.

Neonatally DES-treated female mice showed lower amounts of calcium and phosphorus in pelvis and femur at 12 months of age but not at 2 months of age. The pelvises of 3- to 15-month-old male mice treated neonatally with DES and tamoxifen had lower amounts of calcium and phosphorus than age-matched controls (Figure 1). The femurs of 3- to 15-month-old male mice treated neonatally with tamoxifen, but not with DES, had lower amounts of calcium and phosphorus than age-matched controls (Figure 1). These results indicate that neonatal DES and tamoxifen exposure can result in permanent changes in bone tissue in older male and female mice (*17*).

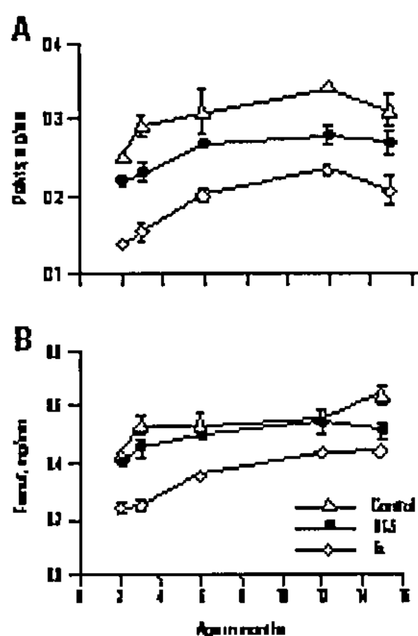

Figure 1. Total amount of calcium per mm length of pelvis (*A*) and femur (*B*) in control, DES-, and tamoxifen (Tx)-treated male mice.

Mouse Anococcygeus Muscle: Sexual Dimorphism and Responsiveness to Steroid Hormones

The anococcygeus muscle described in rats by Gillespie (*28*) is a paired, thin sheet of smooth muscle inserting on the rectum, having a tendinous origin largely on sacral vertebrae (*28,29*). A dense adrenergic innervation is distributed through the muscle along with peptidergic innervation but apparently no cholinergic innervation (*30*). The physiological role of the muscle, however, has not yet been explained.

The rat levator ani muscle from the perineal muscle complex shows sexual dimorphism and its growth is controlled by testosterone (*31*). The rat costo-uterine muscle, which provides a skeletal attachment for the longitudinal myometrial layer of the uterine horn, is also responsive to sex steroids (*32*). The length of the muscle cell increases during pregnancy and after estrogen treatment. However, possible sexual dimorphism and the effect of sex steroids on growth of the anococcygeus muscle have not yet been studied, although it has been reported that the muscle in male rat is bigger than in the female (*33*). The

mouse anoccocygeus muscle was examined for sexual dimorphism, responsiveness to neonatal and postnatal sex hormones including DES, and androgen and estrogen receptor expression.

Cross sections of the anococcygeus muscle of C57BL, ICR and BALB/c mice at 90 days of age showed histology characteristic of smooth muscle. Sexual dimorphism of the muscle was demonstrated in the three mouse strains: the cross-sectional area of the muscle in male mice was significantly larger (1.6 - 3.3 times) than that of females (*34*). Castration significantly reduced the muscle area in male mice. Implantation of a pellet of testosterone increased the muscle area of castrated males. Ovariectomy at 30 days of age increased the muscle area at 60 days of age, but an implantation of estradiol in ovariectomized mice further reduced the muscle area. Estrogen also reduced the muscle area in male mice. Both androgen receptors and estrogen receptors were expressed in the muscle cells until 60 days of age in both sexes.

Neonatal exposure to DES significantly reduced the anococcygeus muscle area in 60-day-old male mice, but strikingly increased (3.1 times) the muscle area in age-matched females. These opposite effects of DES on male and female muscles are surprising. Serum androgen levels in neonatally DES-exposed male mice were not different from those in controls (Fukazawa and Iguchi, unpublished data). The decrease in muscle area seen in neonatally DES-exposed male mice at 60 days of age was not evident if mice were castrated at 30 days of age. The muscle area of neonatally DES-exposed female mice was significantly larger than in controls, and ovariectomy at 30 days of age did not alter this, indicating that the increase in the area by neonatal DES exposure had occurred before 30 days of age and was not affected by later ovarian hormone withdrawal. These results suggest that both androgen and estrogen play an important role in induction of sexual dimorphism of anococcygeus muscle: the muscle is under the control of both androgen and estrogen during the pubertal period, and estrogen (DES) has an irreversible stimulatory effect on the muscle in neonatal female mice.

Conclusions

The study of animals treated perinatally with sex hormones and related compounds provides an opportunity to analyze various factors influencing developmental and carcinogenic processes (*8-12*). Thus, the prenatal and neonatal mouse models continue to indicate possible genital and nongenital changes in human offspring exposed during development to estrogenic hormones, antihormones, and xenobiotics. In further studies, more attention should be paid to abnormalities in nongenital organs exposed to various estrogenic agents during fetal and early postnatal development in mammals including humans.

Reference

1. Takasugi N, Bern HA, DeOme KB. Persistent vaginal cornification in mice. Science 138:438-439 (1962).

2. Takasugi N. Vaginal cornification in persistent estrous mice. Endocrinology 72:607-619 (1963).

3. Dunn TB, Green AW. Cysts of the epididymis, cancer of the cervix, branular cell myoblastoma, and other lesions after estrogen injection in newborn mice. J Natl Cancer Inst 31:425-455 (1963).

4. Takasugi N, Bern HA. Tissue changes in mice with persistent vaginal cornification induced by early postnatal treatment with estrogen. J Natl Cancer Inst 33:855-865 (1964).

5. Takasugi N. Cytological basis for permanent vaginal changes in mice treated neonatally with steroid hormones. Int Rev Cytol 44:193-224 (1976).

6. Forsberg J-G. Developmental mechanism of estrogen-induced irreversible changes in the mouse cervical epithelium. Natl Cancer Inst Monogr 51:41-56 (1979).

7. Mori T, Nagasawa H, Bern HA. Long-term effects of perinatal exposure to hormones on normal and neoplastic mammary growth in rodents--review. J Environ Pathol Toxicol 3:191-206 (1979).

8. Herbst AL, Bern HA, eds. Developmental Effects of Diethylstilbestrol (DES) in Pregnancy. New York:Thieme-Stratton, 1981;203.

9. McLachlan JA, ed. Estrogens in the Environment II: Influences on Development. New York:Elsevier, 1985;435.

10. Mori T, Nagasawa H, eds. Toxicity of Hormones in Perinatal Life. Boca Raton, FL:CRC Press, 1988;184.

11. Bern HA. The fragile fetus. In: Chemically Induced Alterations in Sexual and Functional Development: The Wildlife/Human Connection (Colborn T, Clement C, eds). Princeton, NJ: Princeton Scientific Publishing, 1992;9-16.

12. Iguchi T. Cellular effects of early exposure to sex hormones and antihormones. Int Rev Cytol 139:1-57 (1992).

13. McLachlan JA, Newbold RR, Bullock B. Reproductive tract lesions in male mice exposed prenatally to diethylstilbestrol. Science 190:991-992 (1975).

14. Arai Y, Mori T, Suzuki Y, Bern HA. Long-term effect of perinatal exposure to sex steroids and diethylstilbestrol on the reproductive system of male mammals. Int Rev Cytol 84:235-268 (1983).

15. Iguchi T, Hirokawa M, Takasugi N. Occurrence of genital tract abnormalities and bladder hernia in female mice exposed neonatally to tamoxifen. Toxicology 42:1-11 (1986).

16. Iguchi T, Irisawa S, Uchima F-DA, Takasugi N. Permanent chondrification in the pelvis and occurrence of hernias in mice treated neonatally with tamoxifen. Reprod Toxicol 2:127-134 (1988).

17. Migliacchio S, Newbold RR, Bullock BC, McLachlan JA, Korach KS. Developmental exposure to estrogens induces persistent changes in skeletal tissue. Endocrinology 130:1756-1758 (1992).

18. Uesugi Y, Sato T, Iguchi T. Morphometric analysis of the pelvis in mice treated neonatally with tamoxifen. Anat Rec 235:126-130 (1993).

19. Galand P, Leroy F, Chretien J. Effect of oestradiol on cell proliferation and histological changes in the uterus and vagina of mice. J Endocrinol 49:243-252 (1971).

20. Yamamoto KR. Steroid receptor regulated transcription of specific genes and gene networks. Annu Rev Genet 19:209-252 (1985).

21. Kahn SA, Stancel GM, eds. Protooncogenes and Growth Factors in Steroid Hormone Induced Growth and Differentiation. Boca Raton, FL:CRC Press, 1994;277.

22. Scrocchi LA, Jones LA. Alteration of proto-oncogene *c-fos* expression in neonatal estrogenized BALB/c female mice and murine cervicovaginal tumor LJ6195. Endocrinology 129:2251-2253 (1991).

23. Gardner WU. Sexual dimorphism of the pelvis of the mouse, the effect of estrogenic hormones upon the pelvis and upon the development of scrotal hernias. Am J Anat 59:459-483 (1936).

24. Iguchi T, Irisawa S, Fukazawa Y, Uesugi Y, Takasugi N. Morphometric analysis of the development of sexual dimorphism of the mouse pelvis. Anat Rec 224:490-494 (1989).

25. Uesugi Y, Ohta Y, Asashima M, Iguchi T. Comparative study of sexual dimorphism of the innominate bone in rodents and amphibians. Anat Rec 234:432-437 (1992).

26. Uesugi Y, Taguchi O, Noumura T, Iguchi T. Effects of sex steroids on the development of sexual dimorphism in mouse innominate bone. Anat Rec 234:541-548 (1992).

27. Selmanoff MK, Goldman BD, Ginsburg BE. Developmental changes in serum luteinizing hormone, follicle stimulating hormone and androgen levels in males of two inbred mouse strains. Endocrinology 100:122-127 (1977).